

Effect of polymer ablation on temperature decay of thermal plasmas using induction thermal plasma irradiation technique

メタデータ	言語: eng 出版者: 公開日: 2017-10-03 キーワード (Ja): キーワード (En): 作成者: メールアドレス: 所属:
URL	http://hdl.handle.net/2297/23878

EFFECT OF POLYMER ABLATION ON TEMPERATURE DECAY OF THERMAL PLASMAS USING INDUCTION THERMAL PLASMA IRRADIATION TECHNIQUE

Y Tanaka¹, T Sakuyama¹, D Yamada¹, Y Uesugi¹, S Kaneko², S Okabe²

¹Div. of Electrical Eng. & Computer Sci., Kanazawa Univ., JAPAN. tanaka@ec.t.kanazawa-u.ac.jp

²Eng. R&D Div., Tokyo Electric Power Co., JAPAN.

ABSTRACT

Polymer ablation phenomenon by thermal plasmas was fundamentally investigated using the inductively coupled thermal plasma irradiation technique. It is greatly important to understand interactions between a thermal plasma and polymer materials, for example, for design of low voltage and high voltage circuit breakers. In the present experiment, the Ar induction thermal plasma was directly irradiated to different five kinds of polymer solid bulks. Spectroscopic observation was carried out to measure C₂ spectra, and the C₂ vibrational-rotational temperatures were estimated in different polymer ablated vapors. In addition, the measured mass loss and power loss due to ablation were compared among the different five polymer materials. Results showed that the polymethylene needed the highest power loss for ablation although there is little difference in the vibrational temperatures near the polymer surface among the five polymer materials.

1. INTRODUCTION

In a circuit breaker, an arc plasma is formed between the electrodes during a large current interruption process. Such the arc plasma can contact the gas flow nozzle, and thereby induce ablation of the nozzle made of polymer materials. The polymer ablated vapor affects the interruption capability of the circuit breaker [1]–[7]. On the other hand, in some low-voltage molded case circuit breakers (MCCB), polymer materials are used for the dielectric insulation case or for the quenching chamber wall. These polymer materials may also be ablated by the arc plasma inside the circuit breaker. Recently, a polymer-ablation assisted type of the low-voltage MCCB has been developed [8], and a prototype of polymer-ablation assisted high-voltage gas circuit breaker has been tested [9]. These circuit breakers utilize polymer ablation to raise the pressure in the chamber, and thereby producing strong gas flow or increasing the arc voltage. However, effects of polymer-ablated vapors on arc plasma temperature and other physical plasma parameters are very complicated, and thus those are still insufficiently understood.

In this paper, we fundamentally studied temperature decay of thermal plasmas by polymer ablation using the inductively coupled thermal plasma (ICTP) technique [10]. Use of the ICTP has advantages of no contamination and good controllability. In this experiment, the Ar ICTP was directly irradiated on the bulk of different five kinds of polymer materials; polytetrafluoroethylene (PTFE), polyethylene (PE), polymethylmethacrylate (PMMA), polymethylene (POM), and polyamide-66 (PA66). Spectroscopic observation in polymer ab-

lated vapors was carried out to measure C₂ band spectra, and the C₂ vibrational and rotational temperatures T_{rot} and T_{vib} were determined. In addition, the mass loss and power loss due to ablation were estimated for different five polymer materials from the measured mass after ICTP irradiation. Results show that polymer ablation decreases the temperature near the polymer surface from 9000 to 4000 K for any polymer materials, and that POM has a higher power loss than the other four polymer materials in this work.

2. EXPERIMENTAL SETUP

Fig. 1 shows the plasma torch, the chamber and the specimen holder used in the experiment. The plasma torch is composed of two coaxial quartz tube. Around the torch, an eight-turn induction coil was installed to produce electromagnetic field inside the torch. The frequency of the coil current was 450 kHz. The Ar gas was supplied as a sheath gas along the interior quartz tube. Downstream of this plasma torch, a polymer specimen was located on a stainless steel mount indicated in Fig. 2. The mount with the polymer specimen was further installed on the water-cooled stainless steel specimen holder inside the chamber. The diameter and the thickness of a polymer specimen were 15 mm ϕ and 5 mm, respectively. The distance between the induction coil end and the polymer specimen surface was 200 mm. Spectroscopic observation was carried out to measure C₂ spectra in polymer ablated vapor. Fig. 3 shows observation positions in this work. Observation positions were set at 5.0, 7.5 and 10.0 mm above the polymer specimen surface. At the same time, a high-speed video camera with a band-pass filter was used to measure spatial distribution of radiation intensity from C₂ Swan spectra.

The experimental condition was as follows: The pressure inside the chamber was atmospheric pressure 0.1 MPa. The gas flow rate of Ar was set to 30 slpm (= 5×10^{-5} m³/s). The input power to the thermal plasma was 7.5 kW. In this case, the heat flux onto the surface position of polymers was estimated to be about 0.6 W/mm² (106 W for the whole specimen surface) from the thermofluid calculation. As polymer materials, we treated the following five polymers: PTFE, PE, PMMA, POM, and PA66. Table I summarizes the thermo-chemical properties of the polymers. These properties except the mass density were measured using the thermogravimetry differential thermal analysis (TG-DTA) and the differential scanning calorimetry (DSC) methods. For comparison, a Ti specimen was also used as an irradiated specimen. In case of Ti, no ablation occurs because the Ti specimen is sufficiently cooled by flowing water.

Table I. Thermodynamic properties of polymers.

	PTFE	PE	PMMA	POM	PA66
Mass density [kg/m ³]	2160	932	1163	1410	1140
Melting temperature [K]	618	406	–	435	536
Boiling/thermal decomposition temperature [K]	809	734	618	605	669
Latent heat of melting [kJ/kg]	50.4	191	–	123	62
Latent heat for evaporation [kJ/kg]	936.7	75.5	251.6	1022	222
Specific heat of solid [J/kg/K]	1035	2408	1779	1983	2036
Specific heat of liquid [J/kg/K]	1419	2763	1919	2099	3031

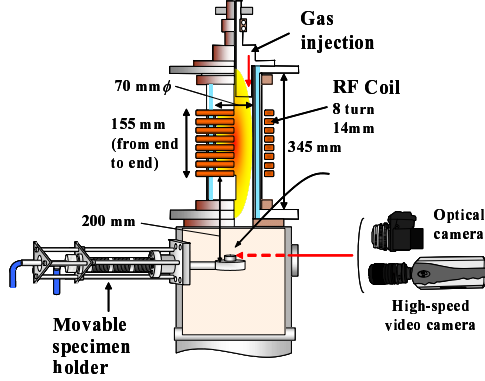


Fig. 1. Plasma torch configuration.

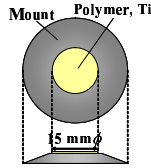


Fig. 2. Mount for specimen.

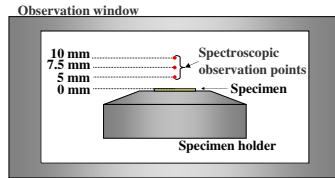


Fig. 3. Spectroscopic observation positions.

3. RESULTS AND DISCUSSIONS

3.1. Spectroscopic observation

Fig. 4 represents an image of ablated vapor from the PTFE surface irradiated by a Ar thermal plasma. This picture was taken using a high-speed video camera with a band-pass filter for C₂ Swan spectra around 467–476 nm [10]. As seen, there is a bright region from the PTFE surface to 10 mm above the surface. This radiation comes from C₂ Swan spectra in the ablated vapor ejected from the PTFE surface.

Figs. 5(a), 5(b) and 5(c) indicate emission spectra measured at 5.0 mm above the specimen surface of PTFE, PE and POM, respectively. For any polymer

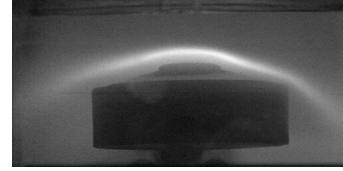


Fig. 4. Image for ablated vapor from PTFE surface irradiated by Ar thermal plasma.

materials, the C₂ Swan system can be apparently observed around 400–600 nm.

3.2. C₂ vibrational and rotational temperatures

The emission coefficient of C₂ Swan spectra can be calculated theoretically if the population of electronically, vibrationally and rotationally excited atoms follows the Boltzmann distribution as follows:

-Emission coefficient:

$$\varepsilon_{n'n''v'v''J'J''} = \frac{hc}{\lambda_{n'n''v'v''J'J''}} N_{n'v'J'} A_{n'n''v'v''J'J''} \quad (1)$$

-Number density of excited molecules:

$$N_{n'v'J'} = \frac{N(T_{ex}, T_{vib}, T_{rot})}{Z(T_{ex}, T_{vib}, T_{rot})} (2J' + 1) \cdot \exp\left(-\frac{hcT_{e'}}{kT_{ex}}\right) \cdot \exp\left(-\frac{hcF_{v'}(J')}{kT_{rot}}\right) \cdot \exp\left(-\frac{hcG_{e'}(v')}{kT_{vib}}\right) \quad (2)$$

-Rotational energy:

$$F_v(J) = B_v J(J+1) - D_v J^2(J+1)^2 \quad (3)$$

-Vibrational energy:

$$G_e(v) = \omega_e \left(v + \frac{1}{2}\right) - \omega_e x_e \left(v + \frac{1}{2}\right)^2 + \omega_e y_e \left(v + \frac{1}{2}\right)^3 \quad (4)$$

-Transition probability

$$A_{n'n''v'v''J'J''} = A_{n'n''} q_{v'v''} \frac{S_{J'}}{2J' + 1} \quad (5)$$

$$A_{n'n''} = \frac{64\pi^4 e^2}{3hc^3 \lambda_{n'n''}^3} |R_{e'n''}|^2 \quad (6)$$

-Hönl-London factor for P, Q and R branches

$$S_{J'}^P = \frac{(J' + 1 + \Lambda')(J' + 1 - \Lambda')}{J' + 1} \quad (7)$$

$$S_{J'}^Q = \frac{(2J' + 1) \Lambda'^2}{J'(J' + 1)} \quad (8)$$

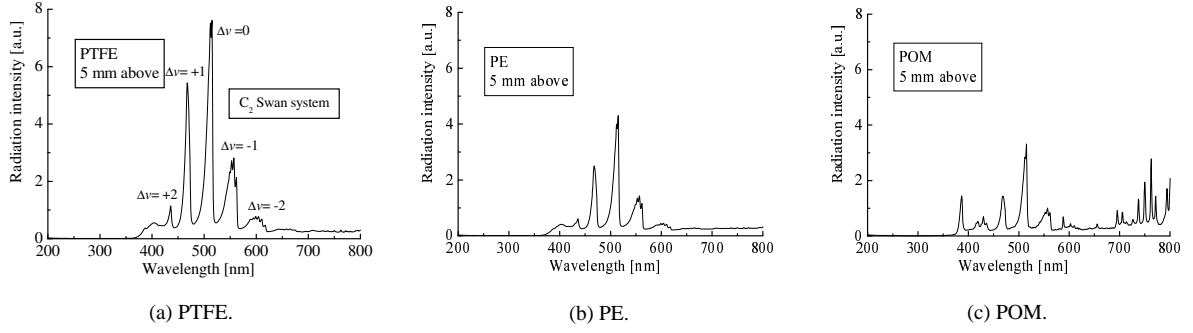


Fig. 5. Spectra measured at 5 mm above polymer specimen irradiated by Ar thermal plasma.

$$S_{J'}^R = \frac{(J' + \Lambda')(J' - \Lambda')}{J'} \quad (9)$$

-Wavenumber

$$\begin{aligned} \nu_{n'n''v'v''J'J''} &= \nu_e + \nu_v + \nu_r \\ &= T_{e'} - T_{e''} + G_e(v') - G_e(v'') \\ &\quad + F_{v'}(J') - F_{v''}(J'') \\ &= \frac{1}{\lambda_{n'n''v'v''J'J''}} \end{aligned} \quad (10)$$

where n, v, J are respectively the quantum numbers for electronic, vibrational and rotational states, $A_{n'n''v'v''J'J''}$: the transition probability from level (n', v', J') to level (n'', v'', J'') , $\lambda_{n'n''v'v''J'J''}$: the wavelength, T_e : the electronic energy, N : the total density of C_2 , Z : the internal partition function, $q_{v'v''}$: Franck-Condon factor, $|R_e^{n'n''}|$: the matrix element of the electronic dipole moment, h : Planck constant, k : Boltzmann constant, c : the speed of light, T_{ex} : the excitation temperature, T_{vib} : the vibrational temperature, T_{rot} : the rotational temperature, B_v, D_v : the rotational constants, $\omega_e, \omega_e x_e, \omega_e y_e$: the vibrational constants, Λ : total orbital angular momentum quantum number.

The temperatures T_{rot} and T_{vib} were determined by fitting the calculated emission coefficient to the measured radiation intensity of C_2 Swan spectra. The calculated emission coefficient was in advance modified by convolution using a measured device function for the spectroscopic observation system to simulate the measured radiation intensity of the C_2 Swan spectra. Fig. 6 shows the axial distribution of T_{rot} and T_{vib} in PTFE ablated vapor. The Ar excitation temperature T_{ex}^{Ar} determined by radiation intensity ratio of two Ar lines was also plotted for an Ti specimen irradiation as no ablation case in the figure for comparison. It is known that the excitation temperature is similar to the electron temperature under the present experimental condition. On the other hand, T_{rot} seems close to the heavy particle temperature because the energy transfer rate between rotational energy levels is enough high by collision with a heavy particle, while T_{vib} is close to the electron temperature rather than the heavy particle temperature since a difference in vibrational levels is as large as 0.1 eV. Thus, we can roughly study decaying rate of the temperature by comparing T_{vib} in polymer

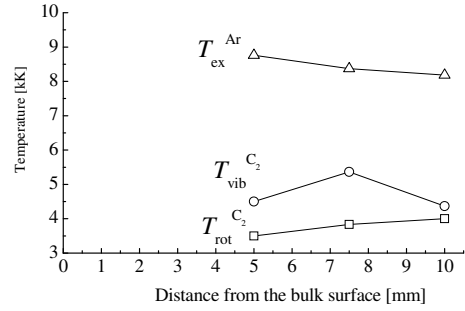


Fig. 6. Axial distribution of estimated vibrational and rotational temperatures in PTFE ablated vapor. Ar excitation temperature without ablation was also plotted for comparison.

ablation case to T_{ex}^{Ar} in no ablation case.

As seen in Fig. 6, if no polymer ablation occurs, Ar excitation temperature was high about 8200–8800 K at 5–10 mm above the surface of the Ti specimen. On the other hand, in the PTFE ablation case, T_{vib} and T_{rot} are by 3500 K lower than T_{ex} at any axial position. This large decay in the temperature may arise from the energy consumption for PTFE solid ablation and the dissociation of PTFE vapor, and also the properties of PTFE vapor.

Fig. 7 indicates the axial distribution of T_{vib} for different polymer materials. For any kind of polymer materials, T_{vib} has a similar value about 4000 K at any axial position. This value is by 3500–4000 K lower than the Ar excitation temperature in no polymer ablation case, and is almost independent of polymer materials in this experimental condition.

3.3. Ablated mass

Strong ablation decreases the mass of the polymer solid specimen to produce ablated vapor, and then pressure rise occurs near the polymer surface. The amount of ablated polymer thus influences the gas flow and temperature decay there. It is therefore important to know the ablated polymer mass, and the resultant polymer vapor volume. We measured the mass loss of the polymer solids after ICTP irradiations every 20 seconds,

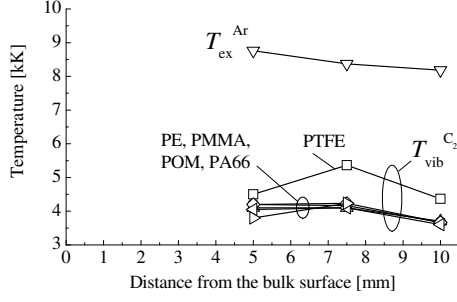


Fig. 7. Axial distribution of estimated vibrational temperature in ablated vapor of different polymer materials. Ar excitation temperature without ablation was added for comparison.

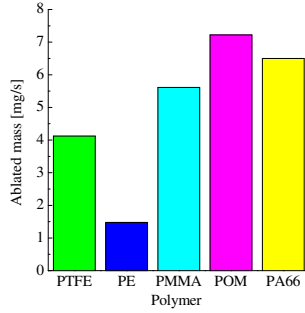


Fig. 8. Ablated mass rate.

and then estimated the averaged ablated polymer mass per second \dot{m}_{pol} .

Fig. 8 shows the ablated polymer mass per second \dot{m}_{pol} . The measurement results indicate that the ablation mass rate for POM is highest whereas the PE has the lowest ablation mass rate.

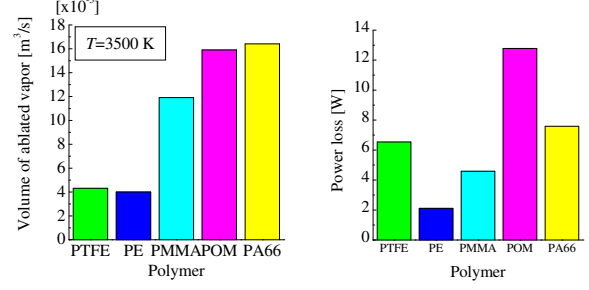
3.4. Ablated vapor volume and power loss by ablation

Ablated vapor causes pressure rise and then produces the gas flow near the surface of ablated solid polymer. To compare the ablated ‘vapor’ amount, ablated vapor volume at atmospheric pressure was estimated using the mass density of the ablated vapor as

$$\dot{V}_{\text{ab}} = \dot{m}_{\text{loss}} / \rho_{3500 \text{ K}} \quad (11)$$

where \dot{V}_{ab} is the ablated vapor volume per second, and $\rho_{3500 \text{ K}}$ is the mass density of polymer vapor at 3500 K. The mass density $\rho_{3500 \text{ K}}$ was derived from the calculated equilibrium composition of ablated polymer vapor at atmospheric pressure. The temperature 3500 K was adopted because the measured T_{rot} and T_{vib} were about 3500 K near any polymer surface due to ablation.

Fig. 9(a) shows the ablated vapor volume at 3500 K. The PTFE and PE have a much lower ablated vapor volume than the others. This means that PTFE and PE may produce much weaker gas flow. On the other hand, PA66 and POM have a large volume of ablated vapor, which can create a strong gas flow near the polymer surface.



(a) Estimated volume of ablated polymer vapor at atmospheric pressure.

(b) Power loss for polymer ablation.

Fig. 9. Estimated ablated volume of polymer and power loss for polymer ablation.

The polymer ablation involves power loss for phase transition from solid to vapor. This power loss may be also related with the temperature decay of the thermal plasma nearby the surface of the ablated polymer. Fig. 9(b) compares the power loss due to ablation. This power loss was estimated from the ablated mass, the latent heat for phase transition and specific heat of solid and liquid polymer indicated in Table I. As seen in this figure, the POM required the highest power loss among the polymers here.

From these above results, POM is found to bring a strong gas flow and higher power loss due to ablation. On the other hand, PE causes weaker gas flow and lower power loss due to ablation among the polymers here.

4. CONCLUSIONS

The polymer ablation phenomena was fundamentally investigated using the induction thermal plasma irradiation technique. Five polymer material such as PTFE, PE, PMMA, POM and PA66 were treated in this paper. It was found that temperature of ablated vapor were about 3500–4000 K for any polymer materials, and that the POM has a larger amount of ablated vapor and a higher power loss than the other four polymer materials in this work.

References

- [1] P Andre, *J. Phys. D: Appl. Phys.*, **30**, 475–93, 1997.
- [2] D J Telfer, et al, *XIV-th Int. Conf. Gas Discharges and their Appl.*, **1**, pp.91–4, 2002.
- [3] J L Zhang, et al, *XIV-th Int. Conf. Gas Discharges and their Appl.* **1** pp.131–4 2002.
- [4] C Luders, et al, *J. Phys. D: Appl. Phys.*, **39**, 666–72, 2006.
- [5] M Seeger, *J. Phys. D: Appl. Phys.* **39** 2180–91, 2006.
- [6] M Seeger, et al, *J. Phys. D: Appl. Phys.* **39** 5016–24, 2006.
- [7] R Kozakov, et al, *J. Phys. D: Appl. Phys.* **40** 2499–506, 2007.
- [8] M Tsukima, et al, *Trans. IEEJ* **122-PE** 969–75, 2002 (in Japanese).
- [9] T Uchii, et al, *Trans. IEEJ*, **124-PE**, 476–84, 2004 (in Japanese).
- [10] Y Tanaka, et al, *J. Phys. D: Appl. Phys.*, **41**, 025203, 2008.